GEOPHYSICAL RESEARCH LETTERS, VOL. 36, L11304, doi:10.1029/2009GL037335, 2009



# Can flash heating of asperity contacts prevent melting?

A. Bizzarri[1]

Received 20 January 2009; revised 20 March 2009; accepted 28 April 2009; published 4 June 2009.

[1] We solve the elasto-dynamic problem for a 3-D rupture, spontaneously propagating on a fault, obeying rate- and state-dependent friction. We explore, through numerical simulations with physically realistic constitutive parameters, the effects on dynamic traction evolution of the flash heating of microscopic asperity contacts. Our results demonstrate that the inclusion of flash heating tends to increase the degree of instability of a homogeneous fault: the supershear rupture regime is favored, significantly larger stress drops are realized and weakening distance and fracture energy increase. We show that the key parameter which controls the temperature evolution and the activation of the flash heating is the slipping zone width, $2w$. We found that for localized shear the rupture exhibits a pulse-like behavior. On the contrary, for large slipping zones, the rupture develops as a sustained crack. Finally, we show that flash heating enhances the onset of melting. **Citation:** Bizzarri, A. (2009), Can flash heating of asperity contacts prevent melting?, *Geophys. Res. Lett.*, *36*, L11304, doi:10.1029/2009GL037335.

## 1. Introduction

[2] Numerical simulations of earthquake ruptures require the introduction of a constitutive law, which describes as realistically as possible the temporal evolution of fault friction and ensures a finite energy flux at the rupture tip. Theoretical studies, laboratory experiments and geological observations revealed that a large number of chemical and physical phenomena can occur within the coseismic time scale, during which the stress release is accomplished and seismic waves are emitted from an earthquake source (see *Bizzarri* [2009, and references therein] for a review).

[3] Among the different mechanisms potentially affecting the evolution fault friction, thermal pressurization of pore fluids [e.g., *Sibson*, 2003; *Bizzarri and Cocco*, 2006a, 2006b, hereinafter referred to as BC06a and BC06b, respectively; *Rice*, 2006] and flash heating (FH thereinafter) of micro-asperity contacts [e.g., *Hirose and Shimamoto*, 2003; *Noda et al.*, 2009, hereinafter referred to as NEA09] have been proved to be the most prominent causes of dramatic traction reduction and have been sometime invoked as a justification of the rarity of melting processes, as suggest by the apparent scarcity of pseudotachylytes [*Sibson*, 2003]. BC06a and BC06b clearly demonstrated that the significant traction reduction induced by thermal pressurization is counterbalanced by an enhanced instability (i.e., greater slip velocities and rupture speed) and that the net effect is that thermal pressurization can not prevent melting when the slipping (or shear) zone, where the slip is concentrated, is sufficiently thin (smaller than few mm).

[4] The aim to this paper is to explore the effects of the FH mechanism on a fully dynamic, 3-D rupture, spontaneously propagating on a planar, homogeneous fault, obeying rate- and state-friction. In particular, we will discuss the effects of FH on rupture velocity, traction evolution, fracture energy, stress drop and onset of melting.

## 2. Model

### 2.1. Numerical Approach

[5] We consider the propagation of a spontaneous earthquake rupture (i.e., without prior imposed rupture velocity) which develops on a finite, isolated, strike slip fault (see Figure S1 of the auxiliary material), embedded in a Hookean isotropic medium initially at the equilibrium.[1] The rupture is fully dynamic, in that the inertia is always accounted for. The solution is performed numerically by using the finite-difference, conventional-grid (FDCG) code of *Bizzarri and Cocco* [2005], which is 2nd-order accurate space and in time and OpenMP-parallelized. In order to reduce computational requests and time we exploit the symmetry about the hypocenter and about the fault plane (see Text S1). The plane $x_3 = 0$ is free of tractions and in the other remaining three planes the Absorbing Boundary Condition described by *Bizzarri and Spudich* [2008] are applied to avoid spurious reflections from the boundaries of the computational domain. The fault is subjected to a constant effective normal stress $\sigma_n^{eff}$ and the rupture is *truly* 3-D, in that both in-plane and anti-plane modes of propagation are considered, with rake rotation allowed.

### 2.2. Fault Governing Law

[6] The fault strength is specified through the introduction of a governing equation, which controls the traction evolution. It is incorporated in the numerical code through the traction-at-spit-node (TSN) scheme, as described by *Bizzarri and Cocco* [2005]. Among the various constitutive equations proposed during the last three decades we will consider the following form of the Ruina-Dieterich (RD henceforth) [*Ruina*, 1983] rate- and state-dependent (RS hereinafter) friction law

$$\begin{aligned} \tau &= \left[\mu_* + a\ln\left(\frac{v}{v_*}\right) + \Theta\right]\sigma_n^{eff} \\ \frac{\mathrm{d}}{\mathrm{d}t}\Theta &= -\frac{v}{L}\left[b\ln\left(\frac{v}{v_*}\right) + \Theta\right] \end{aligned} \tag{1}$$

where $\mu_*$ and $v_*$ are reference parameters for friction coefficient and fault slip velocity modulus $v$, respectively, $a$

[1]Istituto Nazionale di Geofisica e Vulcanologia, Sezione di Bologna, Bologna, Italy.


0094-8276/09/2009GL037335$05.00

[1]Auxiliary materials are available in the HTML. doi:10.1029/2009GL037335.

and $b$ are dimensionless constitutive parameters and $L$ is the characteristic length controlling the temporal evolution of the dimensionless state variable $\Theta$, accounting for the memory effect of previous instability episodes [*Ruina*, 1983].

[7] Recently, the analytical expression for the friction coefficient at velocities typical of earthquake events has been modified to incorporate the FH phenomenon. Since the real contact area of sliding surfaces is smaller than the macroscopic area in contact, the macroscopic fault temperature ($T^f$) changes much more slowly than the temperature on an asperity. This causes the rate of heat production at the local contact to be higher than average the heating rate of the nominal area. As in the models of *Rice* [2006] and NEA09, when sliding velocity $v$ is greater than the critical velocity

$$v_{fh} = \frac{\pi\chi}{D_{ac}}\left(c\frac{T_{weak}-T^f}{\tau_{ac}}\right)^2, \tag{2}$$

FH is activated and the governing law (equation (1)) is modified as described below. In equation (2) $\chi$ is the thermal diffusivity, $c$ the heat capacity for unit volume of the bulk composite, $D_{ac}$ the diameter of asperity contacts, $\tau_{ac}$ their local, unweakened contact strength, and $T_{weak}$ is a constant weakening temperature at which the shear strength of asperities begins to decrease. From equation (2) we have that $v_{fh}$ changes in time as macroscopic fault temperature $T^f$ changes. In a generic fault point $(x_1, x_3)$ and at time $t$, the latter quantity is the solution of the Fourier conduction equation, calculated in the center of a fault structure having a slipping zone of width $2w$ large (BC06a):

$$T^f(x_1,x_3,t) = T_0^f + \frac{1}{2cw}\cdot\int_0^{t-\varepsilon} dt' \operatorname{erf}\left(\frac{w}{2\sqrt{\chi(t-t')}}\right)\tau(x_1,x_3,t')v(x_1,x_3,t') \tag{3}$$

with $T_0^f$ being the initial temperature in the fault center, erf(.) the error function and $\varepsilon$ an arbitrarily small positive real number (see BC06a for details). If velocity overcomes $v_{fh}$ equation (1) are modified into:

$$\begin{aligned}\tau &= \left[\mu_* + a\ln\left(\frac{v}{v_*}\right) + \Theta\right]\sigma_n^{eff}\\ \frac{d}{dt}\Theta &= -\frac{v}{L}\left[\Theta + b\frac{v_{fh}}{v}\ln\left(\frac{v}{v_*}\right) + \left(1-\frac{v_{fh}}{v}\right)\cdot\left(a\ln\left(\frac{v}{v_*}\right) + \mu_* - \mu_{fh}\right)\right]\end{aligned} \tag{4}$$

where $\mu_{fh}$ is a reference parameter of $\mu$ at high $v$ introduced on the basis of the findings of *Beeler et al.* [2008]. The modification of the evolution equation for the state variable at high slip rates results in a different steady state (i.e., for $\dot{\Theta} = 0$) value of friction coefficient: $\mu_{fh}^{ss}(v) = \mu_{fh} + \left[\mu_* - (b-a)\ln\left(\frac{v}{v_*}\right) - \mu_{fh}\right]\frac{v_{fh}}{v}$, instead of $\mu_{lv}^{ss}(v) = \left[\mu_* - (b-a)\ln\left(\frac{v}{v_*}\right)\right]$, retained at low sliding velocities (for $v \le v_{fh}$). In conclusion, depending on the value of $v_{fh}$ in equation (2), the fault locally obeys constitutive equations (1) or (4).

## 3. Effects of Flash Heating on Dynamic Rupture

[8] The parameters adopted in this study, referring to a typical earthquake at 7 km, are summarized in Table 1. In Figure 1 we compare the solutions obtained by adopting the classical RD model (dark gray curves) and the FH model (orange curves) at a target fault point. At $t = 0$ the slip velocity is $v_0 = 1 \times 10^{-4}$ m/s and the fault friction is in its steady state ($\mu_{lv}^{ss}(v_0)\ \sigma_n^{eff} = 70.52$ MPa for parameters of Table 1), as in *Bizzarri et al.* [2001] and *Bizzarri and Cocco* [2005]. At $t = 0$ the state variable is in its steady state ($\Theta^{ss}(v_0) = b\ln\left(\frac{v_*}{v_0}\right) = 0.138$) everywhere except in a circular nucleation patch having radius $r_{nucl} = \frac{7\pi}{24}\frac{GL}{(b-a)\sigma_n^{eff}}$ ($G$ being the rigidity) and center in H, where $\Theta_0 = 1 \times 10^{-4}$.

[9] The introduction of the FH mechanism causes the fault to be more unstable: the rupture accelerates up to supershear rupture velocities, even greater than the Eshelby's speed ($v_E = 4243$ m/s), while with the classical RD law they it remains subshear. From Figures 1a and 1c we can see that both the fault slip velocity peak ($v_{peak}$) and the dynamic stress drop ($\Delta\tau_d$, the difference between peak and minimum level of traction) are greater (nearly 45 and 3.2 times, respectively) than the values obtained without FH. The extremely large values of $v_{peak}$ confirm the 2-D results of NEA09, even if they simulate even larger and more unrealistic values (~300 m/s). We can also see that the crack-like behavior, typical of homogeneous RD law, is altered into a pulse-like solution if we include FH. The time interval where FH is active ($t_{fh} = 36$ ms) is short (nearly 15%) compared to the duration of the pulse ($t_{pulse} = 242$ ms; see Figure 1a); however, it is active for nearly all of the accumulated slip (Figure 1c). The duration of FH is determined by the condition $v \ge v_{fh}$ (see Figure 1a), or equivalently by $t_{died} \ge t_{weak}$ (where $t_{died} = D_{ac}/v$ is the lifetime of an asperity sliding at constant velocity $v$, and $t_{weak} = \frac{\pi\chi}{v^2}\left(c\frac{T_{weak}-T^f}{\tau_{ac}}\right)^2$ is the age at which the asperity is weakened). The modification of the evolution law for the state variable due to FH is responsible for a fast re-strengthening (Figure 1c), which in turn causes the healing of slip. At the end of the rupture the friction coefficient reaches again a steady state in both models (Figure 1b), preventing further failure events (in absence of external loading, as in present models). It is interesting to notice that within the interval $t_{fh}$ the friction coefficient in the FH model is well approximated by the empirical relation provided by *Beeler et al.* [2008] to fit experimental data:

$$\mu^{(Beeler)} = \left\{\mu_{fh} + \mu_* - (b-a)\ln\left(\frac{v}{v_*}\right)\right\} \Big/ \left\{1 + \frac{v}{v_{fh}}\left[1 - e^{-\left(\frac{v}{v_{fh}}\right)^2}\right]\right\}.$$

**Table 1.** Model Discretization and Reference Constitutive Parameters

| Parameter | Value |
|---|---|
| *Medium and Discretization Parameters* | |
| Lamé constants, $\lambda = G$ | 27 GPa |
| S-wave velocity, $v_S$ | 3000 m/s |
| P-wave velocity, $v_P$ | 5196 m/s |
| Cubic mass density, $\rho$ | 3000 kg/m$^3$ |
| Fault length, $L^f$ | 12 km |
| Fault width, $W^f$ | 11.6 km |
| Spatial grid size, $\Delta x_1 = \Delta x_2 = \Delta x_3 \equiv \Delta x$ | 8 m |
| Time step, $\Delta t$ | $4.44 \times 10^{-4}$ s |
| Courant-Friedrichs-Lewy ratio, $\omega_{\mathrm{CFL}} \underset{df}{=} v_S \Delta t/\Delta x$ | 0.1665 |
| *Fault Constitutive Parameters* | |
| Effective normal stress, $\sigma_n^{eff}$ | 120 MPa |
| Logarithmic direct effect parameter, $a$ | 0.016 |
| Evolution effect parameter, $b$ | 0.02 |
| Scale length for state variable evolution, $L$ | $2 \times 10^{-2}$ m |
| Reference value of friction coefficient at low slip rates, $\mu_*$ | 0.56 |
| *Thermal and Flash Heating Parameters* | |
| Initial temperature in the center of the slipping zone, $T_0^f$ | 210°C |
| Heat capacity for unit volume of the bulk composite, $c$ | $3 \times 10^6$ J/(m$^3$ °C) |
| Thermal diffusivity, $\chi$ | $1 \times 10^{-6}$ m$^2$/s |
| Slipping zone thickness, $2w$ | 0.001 m |
| Average diameter of asperities, $D_{ac}$ | 5 $\mu$m |
| Average local shear strength of asperities, $\tau_{ac}$ | 3 GPa |
| Weakening temperature, $T_{weak}$ | 900°C |
| Reference value of friction coefficient at high slip rates, $\mu_{fh}$ | 0.13 |

[10] Even if the stress drop is quite different (Figure 1c), the roll-off near the peak of traction is similar in both models and both exhibit an exponential weakening (confirming 2-D results of NEA09). By defining the equivalent slip-weakening distance $d_0^{eq}$ [*Cocco and Bizzarri*, 2002] as the amount of cumulative slip at which fault traction reaches the 90% of $\Delta\tau_d$ we found values of 0.05 m and 0.075 m, for RD and FH, respectively. Taking additionally into account the difference in stress drop we found that the fracture energy ($E_G = \int_0^{d_0^{eq}} (\tau(u) - \tau(u = d_0^{eq}))\mathrm{d}\,u$; BC06b) in case of FH ($E_G$ = 1.50 MJ/m$^2$) is much larger (nearly 400%) than that obtained in the case of the classical RD model ($E_G$ = 0.383 MJ/m$^2$). Both values are quite comparable with seismic inferences of fracture energy for earthquakes with slip of ~1.1 m ($M_0 = 9.4 \times 10^{17}$ Nm) and 0.3 m ($M_0 = 2.1 \times 10^{17}$ Nm), respectively [*Abercrombie and Rice*, 2005, their Figure 8].

## 4. Temperature Evolution and Melting

[11] In this section we will focus on the temperature change $\Delta T$, defined as the difference between macroscopic fault temperature, $T^f$ (given by equation (3)) and the initial temperature, $T_0^f$. From the numerical experiments discussed in the previous section we have that the reduction in fault traction induced by FH is counterbalanced by the increase in slip velocity, even if this is confined in a short interval. By looking at the black curves in Figure 2b we found that for both FH and classical RD models the temperature rise will cause the melting temperature $T_{melt}$ ($\lessapprox$1500°C) to be reached and exceeded.

[12] Melting occurs also in cases where the fault enters the FH regime later: by considering $T_{weak}$ = 1500°C (the maximum reasonable value for weakening temperature), $v_{fh}$ = 1.05 m/s and therefore the fault remains more in the classical (or low velocity) regime. However, when FH is activated, the fault undergoes extreme instability, as in the reference case (orange curve in Figure S2, corresponding to parameters of Table 1), and $T_{melt}$ is exceeded (see Figure S2b). The same holds if we consider a weaker fault (i.e., a large value of $a$ parameter) and a lower initial and reference values of sliding velocity.

[13] The most prominent parameter controlling the behavior of a rupture where FH is accounted for is the slipping zone thickness, $2w$. In Figure 2 we plot the results of numerical experiments where different values of $2w$ are assumed and cover the range suggested by observations. We emphasize that the value of $2w$ is difficult to quantify, since it exhibits extreme variation along strike, even for a single fault, and because fault zones evolve due to grain size reduction and growth in width by continued slip (A. P. Rathbun and C. Marone, Effect of strain localization on frictional behaviour of sheared granular materials, submitted to *Journal of Geophysical Research*, 2009). By controlling the temporal evolution of $T^f$ (by way of equation (3)) and therefore of $v_{fh}$ (see equation (2)), the slipping zone width finally controls the state of the fault (in terms of $v$, $\tau$ and $\Theta$) at the instant when FH is activated. It also determines whether the solution is pulse-like ($w \leq 5$ mm for parameters of Table 1) or crack-like (see Figure 2a). In the early stage of the rupture the temperature rise is quite similar in all cases, accordingly to the similar evolution of slip velocity up to its peak (Figure 2a). The length of the cohesive zone, where the stress drop is realized, is practically identical in all numerical experiments (Figure 2c), as is the fracture energy. The considered models are definitively undistinguishable also during the accelerating part of the phase portrait (Figure 2d; the only differences are in the re-strengthening phase). Moreover, in the weakening phase, where $\tau$ decreases for increasing $v$, all models clearly exhibit a behavior resembling that of purely velocity-weakening friction law [*Cochard and Madariaga*, 1994].

[14] We emphasize that for a slipping zone larger than 10 mm the fault remains in the FH regime up to the end of the time window; the evolution of the state variable and temperature are such that $v$ always remains in the high velocity regime (i.e., above $v_{fh}$). Moreover, the fault does not heals (the final value of slip velocity is notably greater than $v_0$) and there is no significant fast re-strengthening (Figures 2c and 2d) when $w > 5$ mm. This difference also has clear implications for the temperature evolution; while in self-healing models the temperature reached at the end of the simulation is constant through time, in the crack-like solutions it will increase and it can finally reach $T_{melt}$, since $v$ is constant and non zero (until fault borders are reached and a back-propagating, barrier-healing front destructively interferes with the rupture front). By comparing dashed and full curves in Figure 2b we can conclude that FH generally

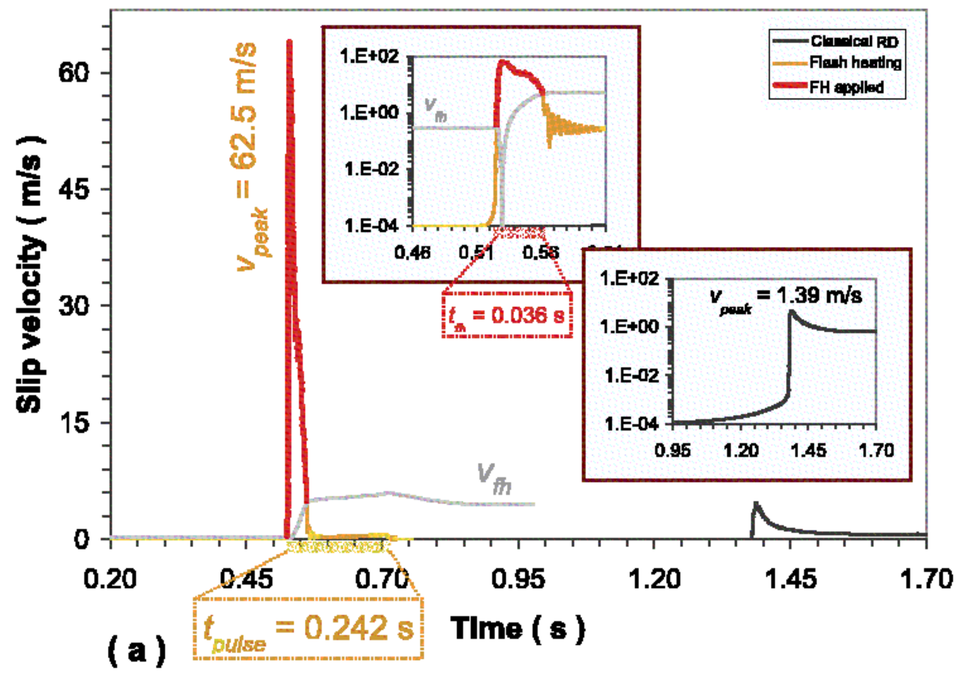


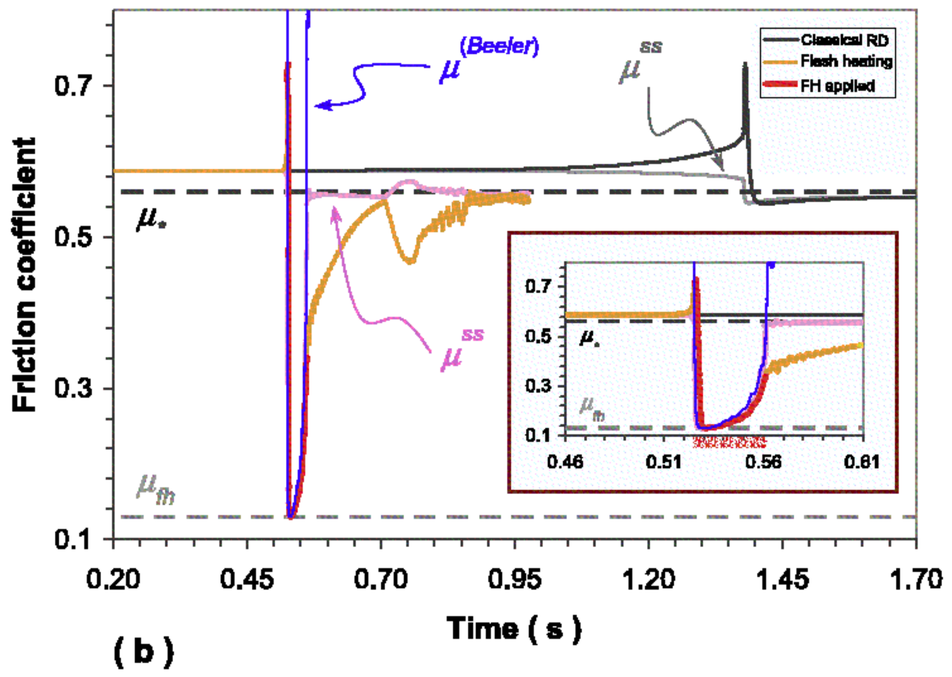


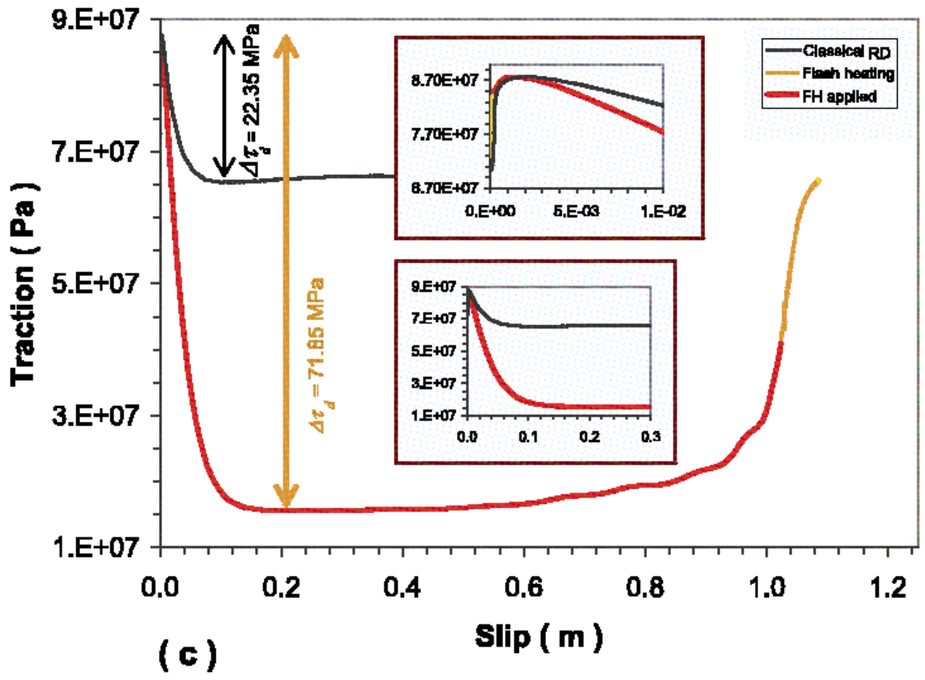


**Figure 1.** Results for a fault obeying the classical RD law (equation (1); dark gray curves) and the RD law with FH of asperity contacts (equation (4); orange curves) at a fault point at the depth of the hypocenter and at a distance of 3 km from it. (a) Slip velocity time history; light gray curve represents $v_{fh}$ (equation (2)) and inset plots are zooms of the peak of $v$. (b) Friction coefficient versus time; steady state friction ($\mu^{ss}$) are superimposed and drawn in gray and pink, respectively; $\mu^{(Beeler)}$ (blue line) is the empirical friction law obtained by *Beeler et al.* [2008] (see text for details). (c) Slip-weakening curve; inset plots are zooms of the roll-off near the peak of traction and of the breakdown phase. In all plots red color denotes the time interval ($t_{fh}$ = 36 ms) where the FH is operating.

enhances the onset of melting. For the same value of fault slip and $2w$, classical RD models, having a crack-like behavior, produce greater temperatures, but FH can not prevent melting (at least for the parameters considered here).

## 5. Discussion and Concluding Remarks

[15] In this paper we have presented numerical experiments of a fully dynamic, *truly* 3-D rupture, spontaneously propagating on a fault obeying rate- and state-friction, with the inclusion of the flash heating (FH) of micro-asperity contacts.

[16] Our results can be summarized as follows: 1) Compared to classical models where FH is neglected, the inclusion of FH considerably increases the degree of instability of the fault; the supershear rupture regime is highly favored, peaks in slip velocity are greater (nearly 50 times), as well as the stress drop (more than 3 times). This is physically reasonable, since a more rapid weakening ought enhance those tendencies. Moreover, the fault traction exhibits larger weakening distances, leading to a greater (nearly 4 times) fracture energies (Figure 1). 2) For highly localized shear the modification of the governing law due to FH causes a fast re-strengthening, leading to a self-healing of slip (Figure 2a). In principle, the transitional value of the size of the slipping zone, discriminating between crack-like and pulse-like solutions, will be sensitive to the adopted ambient stress. We found that for $a$ in between 0.016 and 0.018 $2w \leq 10$ mm causes self-healing. This result extends the findings in 2-D of NEA09; we found here that, for the same value of pre-stress, also $2w$ controls the nature of the rupture (pulse-like or crack-like). In self-healing cases, the strength recovery for increasing slip and slip velocity is quite similar to that previously obtained by *Tinti et al.* [2005] and it is such that the final traction is in a steady state and therefore it is not sufficient to originate a further failure event. 3) The FH increases the propensity of the fault to melt earlier and can not prevent it from occurring (Figure 2b): the decrease of the sliding resistance is counterbalanced by enhanced slip velocities (recall equation (3)). This leaves us with the remaining mystery of why actual evidence of melting is so rare, even if *Kirkpatrick et al.* [2009] recently pointed out the difficulties of preserving and reporting pseudotachylytes in natural faults.

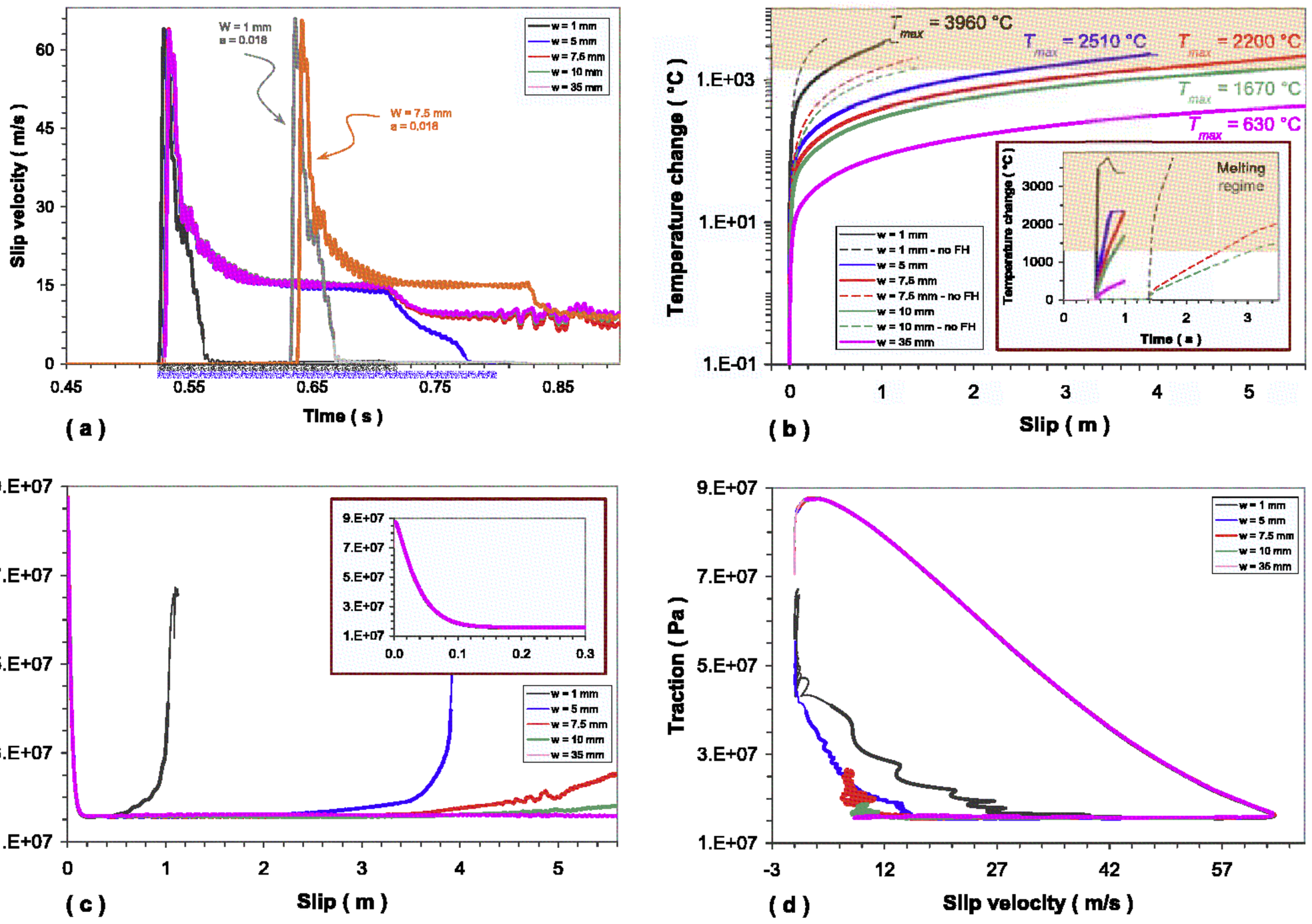


**Figure 2.** Results for different values of the slipping zone thickness $2w$. (a) Fault slip velocity history. (b) Temperature change as a function of cumulative slip, with inset showing the time evolution of temperature change. Dashed lines refer to models without FH. (c) Slip-weakening curve, with inset showing a zoom of cohesive zone. (d) Phase portrait. In all plots thick lines denote the time intervals where the fault is affected by FH. The case $w$ = 1 mm corresponds to the (reference) FH model of Figure 1.

[17] Some of these results are similar to those obtained with thermal pressurization of pore fluids (see for instance BC06a and BC06b). These two phenomena, which are recognized to be the most prominent weakening mechanisms affecting mature faults at cosesimic slip rates, are inherently different; FH is characterized by the length scale of asperity diameter ($D_{ac}$, $\sim$ few $\mu$m (5 $\mu$m in our case)), while the length scale of thermal pressurization is the thermal boundary layer ($\delta = \sqrt{2\chi t_{pulse}} \sim 1$ mm for parameters of Table 1). Moreover, contrary to thermal pressurization, FH does not affects the effective normal stress.

[18] At the same time, both fault models suffer of some limitations: when $T_{melt}$ is reached, Amonton's Law (and consequently classical friction models, as that of equation (1)) is no longer valid. Even if some results have been obtained for the steady state transient [*Nielsen et al.*, 2008], we believe that some additional efforts have to be done in laboratory, in order to better constrain the constitutive behavior in the melting regime and to be able to follow the fault dynamics in the whole range of the temperature developed during a simulated earthquake. Another potential limitation of the model presented in this paper, also common to the thermal pressurization, is the prediction of a nearly fully weakened fault at the end of the breakdown phase. Our present results show stress drops $\sim$70 MPa, which are larger that the typical values of 1–10 MPa [e.g., *Kanamori and Anderson*, 1975].

[19] Finally, we want to remark that the classical formulation of the rate- and state-dependent friction laws basically relies on laboratory measurements where only a fraction of coseismic sliding velocity and normal loading can be attained and where friction force and physical observables are averaged quantities of local, microphysical properties (see *Bizzarri and Cocco* [2006c] for a discussion). Since the microphysics (i.e., at solid-solid contacts) of the sliding layers within the slipping zone is actually missing, temperature and friction are computed on a mathematical fault plane (in the middle of slipping zone), implicitly assuming that they are representative of the macroscopic behavior of the whole $2w$. The modifications of governing equations at high slip rates, as those discussed in this paper, can be regarded as a promising chance to better understand earthquake source physics, combined with new experimental methods based on contact imaging approach [e.g., *Chateauminois and Fretigny*, 2008] and a new generation of laboratory friction machines.

[20] **Acknowledgments.** I would like to thank Eric Dunham for early discussion about general aspects of flash heating and insightful comments by Chris Marone who pointed out the difficulties in constraining the size of the gouge layer in natural faults. Stimulating comments of the Editor, Fabio Florindo, and of two anonymous referees are greatly appreciated.

## References

Abercrombie, R. E., and J. R. Rice (2005), Can observations of earthquake scaling constrain slip weakening?, *Geophys. J. Int.*, *162*, 406–424.

Beeler, N. M., T. E. Tullis, and D. L. Goldsby (2008), Constitutive relationships and physical basis of fault strength due to flash heating, *J. Geophys. Res.*, *113*, B01401, doi:10.1029/2007JB004988.

Bizzarri, A. (2009), What does control earthquake ruptures and dynamic faulting? A review of different competing mechanisms, *Pure Appl. Geophys.*, *166*(5–7), doi:10.1007/s00024-009-0494-1.

Bizzarri, A., and M. Cocco (2005), 3D dynamic simulations of spontaneous rupture propagation governed by different constitutive laws with rake rotation allowed, *Ann. Geophys.*, *48*(2), 277–299.

Bizzarri, A., and M. Cocco (2006a), A thermal pressurization model for the spontaneous dynamic rupture propagation on a three-dimensional fault: 1. Methodological approach, *J. Geophys. Res.*, *111*, B05303, doi:10.1029/2005JB003862.

Bizzarri, A., and M. Cocco (2006b), A thermal pressurization model for the spontaneous dynamic rupture propagation on a three-dimensional fault: 2. Traction evolution and dynamic parameters, *J. Geophys. Res.*, *111*, B05304, doi:10.1029/2005JB003864.

Bizzarri, A., and M. Cocco (2006c), Comment on "Earthquake cycles and physical modeling of the process leading up to a large earthquake," *Earth Planets Space*, *58*, 1525–1528.

Bizzarri, A., and P. Spudich (2008), Effects of supershear rupture speed on the high-frequency content of S waves investigated using spontaneous dynamic rupture models and isochrone theory, *J. Geophys. Res.*, *113*, B05304, doi:10.1029/2007JB005146.

Bizzarri, A., M. Cocco, D. J. Andrews, and E. Boschi (2001), Solving the dynamic rupture problem with different numerical approaches and constitutive laws, *Geophys. J. Int.*, *144*, 656–678.

Chateauminois, A., and C. Fretigny (2008), Local friction at a sliding interface between an elastometer and a rigid spherical probe, *Eur. Phys. J. E.*, *27*, 221–227.

Cocco, M., and A. Bizzarri (2002), On the slip-weakening behavior of rate- and state dependent constitutive laws, *Geophys. Res. Lett.*, *29*(11), 1516, doi:10.1029/2001GL013999.

Cochard, A., and R. Madariaga (1994), Dynamic faulting under rate-dependent friction, *Pure Appl. Geophys.*, *142*, 419–445.

Hirose, T., and T. Shimamoto (2003), Fractal dimension of molten surfaces as a possible parameter to infer the slip-weakening distance of faults from natural pseudotachylytes, *J. Struct. Geol.*, *25*, 1569–1574.

Kanamori, H., and D. L. Anderson (1975), Theoretical basis of some empirical relations in seismology, *Bull. Seismol. Soc. Am.*, *65*, 1073–1095.

Kirkpatrick, J. D., Z. K. Shipton, and C. Persano (2009), Pseudotachylytes: Rarely generated, rarely preserved, or rarely reported?, *Bull. Seismol. Soc. Am.*, *99*, doi:10.1785/0120080114.

Nielsen, S., G. Di Toro, T. Hirose, and T. Shimamoto (2008), Frictional melt and seismic slip, *J. Geophys. Res.*, *113*, B01308, doi:10.1029/2007JB005122.

Noda, H., E. M. Dunham, and J. R. Rice (2009), Earthquake ruptures with thermal weakening and the operation of major faults at low overall stress levels, *J. Geophys. Res.*, doi:10.1029/2008JB006143, in press.

Rice, J. R. (2006), Heating and weakening of faults during earthquake slip, *J. Geophys. Res.*, *111*, B05311, doi:10.1029/2005JB004006.

Ruina, A. (1983), Slip instability and state variable friction laws, *J. Geophys. Res.*, *88*, 10,359–10,370.

Sibson, R. H. (2003), Thickness of the seismic slip zone, *Bull. Seismol. Soc. Am.*, *93*, 1169–1178.

Tinti, E., A. Bizzarri, and M. Cocco (2005), Modeling the dynamic rupture propagation on heterogeneous faults with rate- and state-dependent friction, *Ann. Geophys.*, *48*(2), 327–345.

A. Bizzarri, Istituto Nazionale di Geofisica e Vulcanologia, Sezione di Bologna, Via Donato Creti, 12, I-40128 Bologna, Italy. (bizzarri@bo.ingv.it)